Inductive Heating and E to H Transitions in Capacitive Discharges

P. Chabert,* J.-L. Raimbault, P. Levif, and J.-M. Rax
LPTP, Ecole Polytechnique, 91128 Palaiseau, France

M. A. Lieberman
Department EECS-1770, University of California, Berkeley, California 94720, USA
(Received 5 January 2005; published 7 November 2005)

Capacitive discharges have classically been modeled in the electrostatic approximation. However, electromagnetic effects become significant if the excitation wavelength λ and the plasma skin depth δ are not infinite. An electromagnetic model valid in the entire range of λ and δ of practical interest is solved. We find that the plasma may either be sustained by the usual capacitive (E) field or by an inductive (H) field, and that the discharge experiences E to H transitions as the voltage between the electrodes is raised.

DOI: 10.1103/PhysRevLett.95.205001 PACS numbers: 52.50.Dg, 52.80.−s

Introduction.—Capacitive reactors, widely used for plasma etching in microelectronics [1], have been so far operated in a regime such that the excitation wavelength λ was much greater than the electrode radius, and the plasma skin depth δ was much greater than the plasma thickness, so that the discharge could be modeled as an electrostatic phenomenon. Newly-developed capacitive reactors are larger and driven at higher frequency to reach higher plasma density [2] (a low frequency may be added for independent control of the ion energy [3,4]). Consequently, electromagnetic effects become significant and the electric field has two components; (i) the capacitive field, perpendicular to the electrodes (the E mode), (ii) the inductive field parallel to the electrode (the H mode). Both components can be radially and axially nonuniform due to standing wave and skin effects [5]. In this Letter a transmission line model was derived from the electromagnetic fields, which, coupled to the Child law for the discharge sheaths and to the particle and energy balance, allows one to find a self-consistent solution for the power deposition and the plasma parameters in the entire range of λ and δ of practical interest. The model is the electromagnetic generalization of the lumped-element circuit model classically used for capacitive discharges [1]. Our major conclusion is that capacitive discharges may be inductively sustained, and exhibit E to H transitions as is observed in inductive discharges [6].

Transmission line approach.—We consider a cylindrical plasma reactor with two parallel electrodes of radius R separated by a distance $2l$. The propagation equations for the rf current in the plates I and the voltage between the plates V, are

$$\frac{dV}{dr} = -Z'I(r), \tag{1}$$

$$\frac{dI}{dr} = -Y'V(r). \tag{2}$$

Here, $Z' = R'_{\rm ind} + jL'\omega$, $Y'^{-1} = R'_{\rm cap} + R'_i + (jC'\omega)^{-1}$, where L', C', $R'_{\rm ind}$, $R'_{\rm cap}$, and R'_i are, respectively, the series inductance, parallel capacitance, and resistances per unit length which will be computed from the electromagnetic fields in the following. These transmission line elements are nonlinear since they depend on the local voltage $V(r)$ and density $n_e(r)$. In order to find a self-consistent solution, we must couple the transmission line equations to the particle and power balance equations. In this Letter, we treat the low-pressure case, where the electron density radial profile is determined by nonlinear diffusion with constant ionization (in the high-pressure case, the radial profile is determined by the local power deposition). A good fit of the low-pressure solution of Godyak [7] is given by

$$n_e(r) = n_{\rm e0}\left[1 - (1 - h_R^2)\frac{r^2}{R^2}\right]^{1/2}, \tag{3}$$

where $h_R = 0.80(4 + R/\lambda_i)^{-1/2}$ is the radial edge-to-center density ratio. Here $\lambda_i = (n_g\sigma_i)^{-1}$ is the ion mean free path, with n_g as the gas density and $\sigma_i \approx 10^{-18}$ m^2 for argon. The density at the reactor center, $n_{\rm e0}$, is determined from the global electron power balance $P_e = P_{\rm loss}$ where

$$P_e = \frac{1}{2}\int_0^R R'_{\rm cap}\left|\frac{dI}{dr}\right|^2 dr + \frac{1}{2}\int_0^R R'_{\rm ind}|I|^2 dr \tag{4}$$

is the absorbed power, which includes capacitive heating (first term) and inductive heating (second term), and $P_{\rm loss} = 2n_{\rm e0}u_B(\pi R^2 h_l + 2\pi R d h_R)\varepsilon_T$ is the loss power. Here, ε_T is the total energy loss per electron-ion pair created, $u_B = (eT_e/M)^{1/2}$ is the Bohm velocity with M the ion mass. $h_l = 0.86(3 + d/\lambda_i)^{-1/2}$ is the axial plasma edge-to-center density ratio, and $d = l - s$ is the plasma half-width, with s the sheath width. The power loss is a function of T_e, which is determined by the particle balance, $n_g K_{\rm iz}\pi R^2 d = u_B(\pi R^2 h_l + 2\pi R d h_R)$, where $K_{\rm iz}$ is the ionization coefficient given in [8].

For a symmetrically driven system, the boundary conditions are $V(r = 0) = V_0$ and $I(r = 0) = 0$ (a standing wave with no edge effects at $r = R$). In practice, the model is solved as follow: for a given V_0 and a set of $n_{\rm e0}$ values,

we successively: (i) calculate T_e from the particle balance equation, (ii) insert $n_e(r)$ into the Child law (Eq. 42 in [8]) to obtain the sheath width $s(r, V)$, (iii) solve the transmission line equations to obtain $V(r)$ and $I(r)$, (iv) calculate P_e and P_{loss}, and plot both versus n_{e0}, the intersection of the two curves being the equilibrium.

Field equations.—To compute the distributed circuit parameters, we locally model the plasma, separated from the electrodes by two sheaths, as a uniform dielectric stationary in time having a complex relative permittivity $\kappa_p = 1 - \omega_p^2/[\omega(\omega - j\nu_m)]$, where $\omega_p = (e^2 n_e/\varepsilon_0 m_e)^{1/2}$ is the plasma frequency and ν_m is the electron-neutral elastic collision frequency. This model is justified because, although each sheath oscillates in width, the oscillations are 180° out of phase. Therefore the total sheath width, and thus the sheath capacitance, is roughly constant in time. Assuming an azimuthal magnetic field H_ϕ, the corresponding components of the electric field, E_z and E_r, are determined from Maxwell's equations. The propagation equation for H_ϕ in the plasma and sheath regions is

$$\frac{\partial^2 H_\phi}{\partial z^2} + \frac{\partial^2 H_\phi}{\partial r^2} + \frac{1}{r}\frac{\partial H_\phi}{\partial r} + \left(k_0^2\kappa - \frac{1}{r^2}\right)H_\phi = 0, \quad (5)$$

where $\kappa = \kappa_p$ in the plasma and $\kappa = 1$ in the sheaths, and $k_0 = \omega/c$ is the free space wave number. Considering only the waves traveling radially outward (cylindrical geometry), we search for solutions having the form $H_\phi(r, z, t) = \text{Re}[\tilde{H}_\phi(z) H_1^{(2)}(kr) e^{j\omega t}]$, where $H_1^{(2)}(kr)$ is the Hankel function of the second kind [9]. Since $\tilde{E}_r = 0$ at $z = 0$ and $z = \pm l$, and both $\tilde{E}_r$ and $\tilde{H}_\phi$ are continuous at $z = \pm d$, the fields in the plasma are

$$\tilde{E}_r(z) = -\frac{A\alpha_p \cosh\alpha_0 s}{j\omega\varepsilon_0\kappa_p}\sinh\alpha_p z, \quad (6)$$

$$\tilde{H}_\phi(z) = A\cosh\alpha_0 s\cosh\alpha_p z, \quad (7)$$

$$\tilde{E}_z(z) = \frac{Ak\cosh\alpha_0 s}{j\omega\varepsilon_0\kappa_p}\cosh\alpha_p z. \quad (8)$$

Similarly, the fields in the sheath regions are

$$\tilde{E}_r = \frac{A\alpha_0\cosh\alpha_p d}{j\omega\varepsilon_0}\sinh\alpha_0(l - z), \quad (9)$$

$$\tilde{H}_\phi = A\cosh\alpha_p d\cosh\alpha_0(l - z), \quad (10)$$

$$\tilde{E}_z = \frac{Ak\cosh\alpha_p d}{j\omega\varepsilon_0}\cosh\alpha_0(l - z). \quad (11)$$

We have introduced the wave number k along r, and the wave numbers $\alpha_{p,0}$ along z in the plasma and in the sheath, respectively, with $k^2 - \alpha_p^2 = k_0^2\kappa_p$ and $k^2 - \alpha_0^2 = k_0^2$. In the regime of interest $|\alpha_0 s| \ll 1$ and $|k\delta| \ll 1$. If we additionally assume that $\nu_m \ll \omega \ll \omega_p$, then $\alpha_p \approx 1/\delta$, and the dispersion relation of the surface wave is simply

$$k^2 \approx k_0^2\left[1 + \frac{\delta}{s}\tanh\frac{d}{\delta}\right] \quad (12)$$

where we have introduced $\delta \equiv c/\omega_p$, the inertial plasma skin depth. Equation (12) is valid if $(\omega_p/\omega)^2 \gg \max(1 + d/s, s/\delta)$, a condition satisfied from small to large skin depth.

Distributed circuit parameters.—For TM modes, the voltage and current in the transmission line are usually calculated from the power flow of the traveling wave [9]. However, from (6)–(11) in the regime of interest, the electric field in the sheaths is nearly transverse (quasi-TEM) and is much greater than that in the plasma. In this case, the voltage amplitude for a single radially propagating wave is approximately $\tilde{V} = -2\int_0^l \tilde{E}_z(z)dz$, the current amplitude is $\tilde{I} = 2\pi r\tilde{H}_\phi(z = l)$, and the characteristic impedance of the line is $\tilde{V}/\tilde{I} = \sqrt{L'/C'}$. In addition, we have $k = \omega\sqrt{L'C'}$, so that we can solve for L' and C' using (12), to obtain

$$L' = \mu_0\frac{s}{\pi r}\left(1 + \frac{\delta}{s}\tanh\frac{d}{\delta}\right)\left(1 - \frac{\omega^2}{\omega_p^2}\frac{\delta}{s}\tanh\frac{d}{\delta}\right) \quad (13)$$

and

$$C' = \frac{\varepsilon_0\pi r}{s}\left(1 - \frac{\omega^2}{\omega_p^2}\frac{\delta}{s}\tanh\frac{d}{\delta}\right)^{-1}. \quad (14)$$

The second terms in the last brackets of (13) and (14) will be neglected in the following since $\omega \ll \omega_p$. When δ is large, (13) reduces to its value in vacuum, as expected.

The resistances in (1) and (2) are calculated from the power dissipation. The power loss per unit length due to the inductive $\tilde{E}_r(z)$ field is $\text{Re}[\int_0^d \tilde{J}_r(z)\tilde{E}_r^*(z)dz]2\pi r = \frac{1}{2}|\tilde{I}|^2 R'_{\text{ind}}$, which yields the series transmission line resistance per unit length,

$$R'_{\text{ind}} = \frac{1}{2\pi r\sigma_{\text{dc}}\delta}\left[\frac{\sinh(2d/\delta) - (2d/\delta)}{1 + \cosh(2d/\delta)}\right], \quad (15)$$

where $\sigma_{dc} = (e^2 n_e/m_e\nu_m)$ is the dc plasma conductivity. When the skin depth is large ($n_e \to 0$), R'_{ind} increases linearly with n_e, whereas when $n_e \to \infty$, R'_{ind} decreases as $1/n_e^{1/2}$. This is similar to the plasma resistance of a classical inductive discharge driven by a coil through a dielectric window. The inductive stochastic heating [10] may be incorporated using an effective collision frequency $\nu_{\text{eff}} = \nu_m + \nu_{\text{stoc}}$ [1].

The parallel resistance due to Ohmic heating by the capacitive field $\tilde{E}_z(z)$ is found similarly,

$$R'_{\text{ohm}} = \frac{\delta}{2\pi r\sigma_{\text{dc}}}\left[\frac{\sinh(2d/\delta) + 2d/\delta}{1 + \cosh(2d/\delta)}\right]. \quad (16)$$

Unlike the inductive resistance, R'_{ohm} always decreases with n_e. At low pressure, Ohmic heating is dominated by stochastic heating and Ohmic heating in the sheath, which are both independent of skin effects since they occur within the sheath region. From [8] we introduce the following

resistances to account for these power dissipations

$$R'_{\mathrm{stoc}} = 1.8 \times \frac{(mT_e)^{1/2} s^2}{e^{1/2} \varepsilon_0 \pi r |V|}, \tag{17}$$

$$R'_{\mathrm{ohm,sh}} = \frac{m \nu_m s^3}{e \varepsilon_0 \pi r |V|}. \tag{18}$$

Let us note that an alternative model for collisionless heating has been proposed by Turner and co-workers [11,12]. This model would lead to an approximately 40% decrease in the stochastic resistance, but would not modify the main conclusions of this Letter. We must also include the resistance due to power dissipation by ions flowing in the sheaths [8],

$$R'_i = 3.32 \times \frac{e h_l n_e u_B s^2}{\omega^2 \varepsilon_0^2 \pi r |V|}. \tag{19}$$

Finally, $R'_{\mathrm{cap}} = R'_{\mathrm{ohm}} + R'_{\mathrm{stoc}} + R'_{\mathrm{ohm,sh}}$.

Results.—Typical power versus n_{e0} graphs are shown in Fig. 1 at 30 mTorr, 200 MHz, with electrodes of radius $R = 15$ cm spaced by $2l = 4$ cm, for (a) $V_0 = 60$ V and (b) $V_0 = 800$ V. At low voltage, capacitive heating dominates (E mode), whereas at high voltage the inductive heating takes over (H mode), such that the discharge experiences an E to H transition as the voltage is raised. Unlike in inductive discharges, the transition is smooth and is not clearly defined. For the sake of simplicity, we will define the E to H transition as the condition $P_{\mathrm{ind}} = P_{\mathrm{cap}}$. The equilibrium electron density is plotted as a function of V_0 in Fig. 2 for the same parameters as in Fig. 1, for (a) 60 and (b) 200 MHz. At 60 MHz, the transition is never reached whereas at 200 MHz, it occurs at $V_0 = 420$ V, when $n_{e0} = 6 \times 10^{17}$ m^{-3}. Hence, the transition does not occur at a specific electron density, but also depends on the frequency. The dashed line represents the equilibrium electron density calculated with capacitive heating only, showing that at high frequency the error may be significant if inductive heating is ignored.

Before examining the role of the driving frequency, let us recall that the voltage and the current are not radially uniform due to the standing wave effect. The voltage is maximal in the center, where the current is zero, and decreases as r increases. The radial position where the voltage reaches its minimum (and the current its maximum) will be denoted $r = R_1 \approx \lambda/4$ in the following. The standing wave effect is weak if $R_1 \gg R$, and strong if $R_1 \leq R$.

The ratio of inductive-to-capacitive power, $P_{\mathrm{ind}}/P_{\mathrm{cap}}$, is plotted in Fig. 3 as a function of n_{e0}, at equilibrium (n_{e0} was varied by varying V_0), for various frequencies. Let us first discuss the case $R = 0.15$ m, for which the standing wave effect is moderate ($R_1 > R$). The inductive heating is barely seen at 27 MHz but it increases significantly with the frequency; E to H transitions are obtained for frequencies above 170 MHz. The frequency dependence can be understood from a simplified analytical solution obtained for $R_1 \gg R$, neglecting the spatial variations of the electron density and the voltage; $n_e(r) = n_{e0}$ and $V(r) = V_0$. Assuming that $R'_{\mathrm{cap}} \approx R'_{\mathrm{stoc}}$ (a very good approximation), the ratio at equilibrium is given by

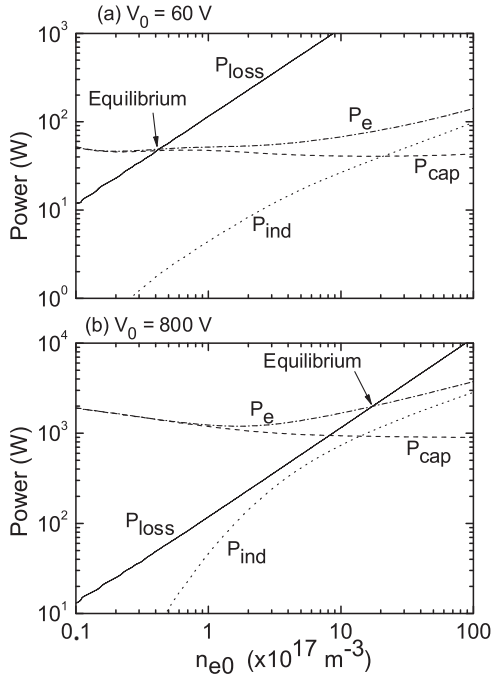

FIG. 1. Absorbed and loss power versus n_{e0} for a 30 mTorr, 200 MHz capacitive discharge with electrodes of radius $R = 15$ cm separated by $2l = 4$ cm, for (a) $V_0 = 60$ V and (b) $V_0 = 800$ V.

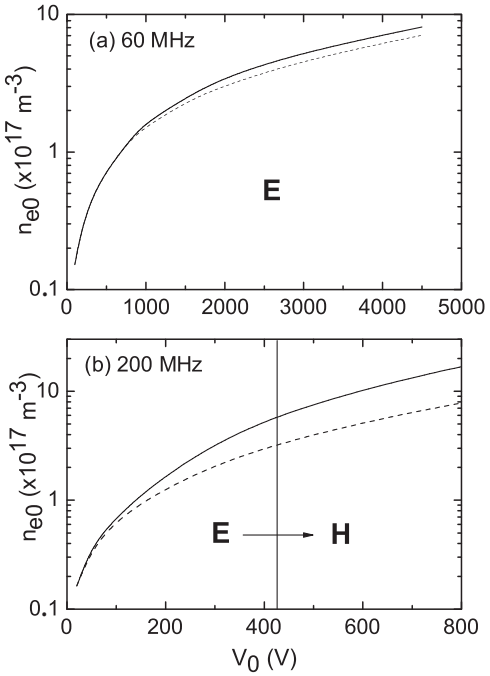

FIG. 2. Electron density versus V_0 for the same parameters as in Fig. 1, for (a) 60 and (b) 200 MHz; the dashed line gives the density if inductive heating is ignored.

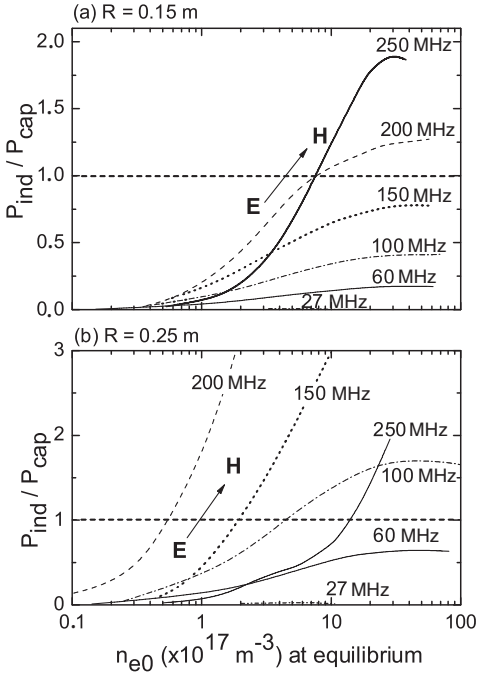

FIG. 3. Inductive-to-capacitive power ratio, $P_{\mathrm{ind}}/P_{\mathrm{cap}}$, versus n_{e0} at equilibrium, for several frequencies, and for (a) $R = 15$ cm and (b) $R = 25$ cm.

$$\frac{P_{\mathrm{ind}}}{P_{\mathrm{cap}}} \propto \nu_m h_l^{1/2} R^2 \omega \left[\frac{\sinh(2d/\delta) - 2d/\delta}{1 + \cosh(2d/\delta)}\right] \qquad (20)$$

in the limit of small inductive heating, $P_{\mathrm{ind}} \ll P_{\mathrm{cap}}$. This approximate formula explains most of the variations shown in Fig. 3(a). At given density, the inductive heating indeed increases with the frequency and, if the frequency is fixed, the ratio increases with n_{e0} at low density and saturates at high density. Equation (20) also predicts that inductive heating will increase with the electrode radius. This is well verified as long as the standing wave effect remains weak (compare 60 MHz at $R = 0.15$ and at $R = 0.25$).

The situation becomes more complicated when the standing wave effect is strong, $R_1 \leq R$. For instance, we note in Fig. 3(b) that $P_{\mathrm{ind}}/P_{\mathrm{cap}}$ is smaller at 250 MHz than at 150 MHz, in contradiction with the above discussion. To understand the regime of a strong standing wave, we plot in Fig. 4 the ratio $P_{\mathrm{ind}}/P_{\mathrm{cap}}$ versus frequency for a fixed equilibrium density $n_{e0} = 5 \times 10^{17}$ m^{-3}. The ratio increases with frequency while $R_1 \geq R$, reaches its maximum when $R_1 \approx R$ (in fact a little after), and decays for $R_1 \leq R$. This is because when $R_1 \leq R$, the voltage has a node and increases again for $r \geq R_1$, as does the capacitive heating, and the current decreases for $r \geq R_1$, as does the inductive heating.

Conclusion.—We have shown that capacitive discharges may be sustained by an inductive field and that smooth E to H transitions occur when the voltage between the electrodes is raised. For conditions when the standing wave effect is moderate, i.e., when there is no voltage node for $r < R$, the ratio of inductive-to-capacitive heating increases with the frequency and/or the electrode radius. We have studied the low-pressure regime where the power deposition is nonlocal, so that the E to H transitions are global. However, the power deposition will be local at high pressure, inducing spatial E to H transitions with the center of the discharge being in the E mode, while the edges are in the H mode. This phenomenon was probably experimentally observed by Perret *et al.* [13].

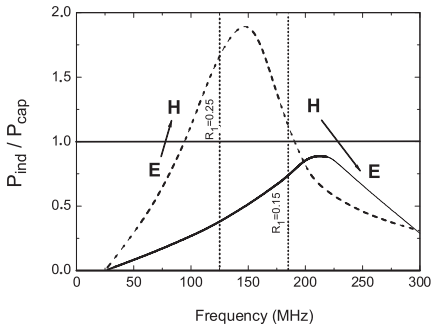

FIG. 4. Inductive-to-capacitive power ratio, $P_{\mathrm{ind}}/P_{\mathrm{cap}}$, versus frequency for $n_{e0} = 5 \times 10^{17}$ m^{-3}. The dashed line is for $R = 0.25$ m and the solid line is for $R = 0.15$ m.

M. A. L. gratefully acknowledges the support provided by LPTP at Ecole Polytechnique, the State of California MICRO program, National Science Foundation Grant No. ECS-0139956, and a State of California UC Discovery Grant from the Industry-University Cooperative Research Program.

*Electronic address: chabert@lptp.polytechnique.fr

[1] M. Lieberman and A. Lichtenberg, *Principles of Plasma Discharges and Materials Processing* (Wiley, New York, 2005), 2nd ed.
[2] A. Perret, P. Chabert, J. Jolly, and J.-P. Booth, Appl. Phys. Lett. **86**, 021501 (2005).
[3] J. Robiche, P. C. Boyle, M. M. Turner, and A. R. Ellingboe, J. Phys. D: Appl. Phys. **36**, 1810 (2003).
[4] H. Kim and J. Lee, Phys. Rev. Lett. **93**, 085003 (2004).
[5] M. A. Lieberman, J.-P. Booth, P. Chabert, J.-M. Rax, and M. M. Turner, Plasma Sources Sci. Technol. **11**, 283 (2002).
[6] M. M. Turner and M. A. Lieberman, Plasma Sources Sci. Technol. **8**, 313 (1999).
[7] V. Godyak, *Soviet Radiofrequency Discharge Research* (Delphic Associates, Falls Church, VA, 1986).
[8] P. Chabert, J.-L. Raimbault, J.-M. Rax, and M. Lieberman, Phys. Plasmas **11**, 1775 (2004).
[9] S. Ramo, J. Whinnery, and T. V. Duzer, *Fields and Waves in Communication Electronics* (Wiley, New York, 1965).
[10] M. Turner, Phys. Rev. Lett. **71**, 1844 (1993).
[11] M. Turner, Phys. Rev. Lett. **75**, 1312 (1995).
[12] G. Gozadinos, M. M. Turner, and D. Vender, Phys. Rev. Lett. **87**, 135004 (2001).
[13] A. Perret, P. Chabert, J.-P. Booth, J. Jolly, J. Guillon, and P. Auvray, Appl. Phys. Lett. **83**, 243 (2003).